Electronic Supplementary Information

Synthesis of platinum(II)-complex end-tethered polymers: Spectroscopic properties and nanostructured particles

Shengchao Qiu,[a] Hua Xue,[a] Ran Wang,[a] Chi Zhang,[a] Qun He,*[a] Guanjun Chang[b] and Weifeng Bu*[ac]

[a] State Key Laboratory of Applied Organic Chemistry, Key Laboratory of Nonferrous Metals Chemistry and Resources Utilization of Gansu Province, and College of Chemistry and Chemical Engineering, Lanzhou University, Lanzhou, 730000, China.
[b] State Key Laboratory of Solid Lubrication, Lanzhou Institute of Chemical Physics, Chinese
[c] Academy of Sciences, Lanzhou, 730000, China. State Key Laboratory of Solid Lubrication, Lanzhou Institute of Chemical Physics, Chinese Academy of Sciences, Lanzhou, 730000, China
Email: hequn@lzu.edu.cn; buwf@lzu.edu.cn

EXPERIMENTAL SECTION

Measurements.

[1] H NMR spectra were recorded on a JNM-ESC400 instrument, in which tetramethylsilane (TMS) was used as an internal standard and d-chloroform ($CDCl_3$) as a solvent. Matrix-assisted laser desorption/ionization time-of-flight (MALDI-TOF) mass spectra were performed on a Bruker ultraflextreme. Gel permeation chromatography (SEC) experiments were recorded on a Waters 1515 instrument and the values of number-average molecular weight (M_n), weight-average molecular weight (M_w), and polydispersity index ($Đ$) of **PS*n*L-I**, and **PS*n*L-II** were determined using polystyrene as a calibration standard. Tetrahydrofuran (THF) was used as eluent at a flow rate of 1.0 mL/min and the column temperature was controlled to be 40 °C. Fourier transformation infrared (FT-IR) spectra experiments were recorded on a Nicolet NEXUS 670. UV-vis absorption spectra were carried out using a SHIMADZU UV-2550 spectrophotometer. All luminescence measurements were made using a Hitachi-7000 spectrofluorometer. The diameters (D_h) of particles in chloroform/methanol mixed solvent was obtained using a dynamic light scattering (DLS) instrument performed on a Brookhaven 90Plus Pals spectrometer. Transmission electron microscopy (TEM) experiments were conducted on an FEI Talos F200s operating at 200 kV. All measurements were carried out at room temperature except for SEC experiments.

Characterization Details

PS$_{14}$L-I: Yield: 198 mg, 90%. ^{1}H NMR (400 MHz, $CDCl_3$): δ 8.37 (t, J = 8.0 Hz, 2H, Ar), 8.06 (t, J = 8.0 Hz, 1H, Ar), 7.87 (d, J = 8.0 Hz, 2H, Ar), 7.46 (d, J = 8.0 Hz, 2H, Ar), 7.36 (m, 4H), 6.36 – 7.08 (br, 70H, $-C_6H_5$), 5.11 (m, 1H, −ArCH−), 4.77 (t, J = 7.4 Hz, 2H, $-NCH_2-$), 4.19 (s, 3H, $-NCH_3$), 3.93 (t, J = 6.5 Hz, 2H, $-OCH_2-$), 3.63 (m, 2H, $-CH_2-$) 1.25 – 2.18 (br, 65H, $-CH_2-$, $-CHCH_2-$). $M_{n,NMR}$ = 2200 g mol^{-1}, $M_{n,SEC}$ = 2000 g mol^{-1}, $Đ$ = 1.11.

PS$_{19}$L-I: Yield: 252 mg, 90%. ^{1}H NMR (400 MHz, $CDCl_3$): δ 8.37 (t, J = 8.0 Hz, 2H, Ar), 8.06

(t, J = 8.0 Hz, 1H, Ar), 7.87 (d, J = 8.0 Hz, 2H, Ar), 7.46 (d, J = 8.0 Hz, 2H, Ar), 7.36 (m, 4H), 6.36 – 7.08 (br, 95H, $-C_6H_5$), 5.11 (m, 1H, −ArCH−), 4.77 (t, J = 7.4 Hz, 2H, $-NCH_2-$), 4.19 (s, 3H, $-NCH_3$), 3.93 (t, J = 6.5 Hz, 2H, $-OCH_2-$), 3.63 (m, 2H, $-CH_2-$) 1.25 – 2.18 (br, 79H, $-CH_2-$, $-CHCH_2-$). $M_{n,NMR}$ = 2800 g mol^{-1}, $M_{n,SEC}$ = 2600 g mol^{-1}, $Đ$ = 1.06.

PS_{24}L-I: Yield: 310 mg, 91%. ^{1}H NMR (400 MHz, $CDCl_3$): δ 8.37 (t, J = 8.0 Hz, 2H, Ar), 8.06 (t, J = 8.0 Hz, 1H, Ar), 7.87 (d, J = 8.0 Hz, 2H, Ar), 7.46 (d, J = 8.0 Hz, 2H, Ar), 7.36 (m, 4H), 6.36 – 7.08 (br, 120H, $-C_6H_5$), 5.11 (m, 1H, −ArCH−), 4.77 (t, J = 7.4 Hz, 2H, $-NCH_2-$), 4.19 (s, 3H, $-NCH_3$), 3.93 (t, J = 6.5 Hz, 2H, $-OCH_2-$), 3.63 (m, 2H, $-CH_2-$) 1.25 – 2.18 (br, 95H, $-CH_2-$, $-CHCH_2-$). $M_{n,NMR}$ = 3200 g mol^{-1}, $M_{n,SEC}$ = 3300 g mol^{-1}, $Đ$ = 1.10.

PS_{34}L-I: Yield: 391 mg, 91%. ^{1}H NMR (400 MHz, $CDCl_3$): δ 8.37 (t, J = 8.0 Hz, 2H, Ar), 8.06 (t, J = 8.0 Hz, 1H, Ar), 7.87 (d, J = 8.0 Hz, 2H, Ar), 7.46 (d, J = 8.0 Hz, 2H, Ar), 7.36 (m, 4H), 6.36 – 7.08 (br, 170H, $-C_6H_5$), 5.11 (m, 1H, −ArCH−), 4.77 (t, J = 7.4 Hz, 2H, $-NCH_2-$), 4.19 (s, 3H, $-NCH_3$), 3.93 (t, J = 6.5 Hz, 2H, $-OCH_2-$), 3.63 (m, 2H, $-CH_2-$) 1.25 – 2.18 (br, 125H, $-CH_2-$, $-CHCH_2-$). $M_{n,NMR}$ = 4300 g mol^{-1}, $M_{n,SEC}$ = 4300 g mol^{-1}, $Đ$ = 1.07.

PS_{41}L-I: Yield: 460 mg, 92%. ^{1}H NMR (400 MHz, $CDCl_3$): δ 8.37 (t, J = 8.0 Hz, 2H, Ar), 8.06 (t, J = 8.0 Hz, 1H, Ar), 7.87 (d, J = 8.0 Hz, 2H, Ar), 7.46 (d, J = 8.0 Hz, 2H, Ar), 7.36 (m, 4H), 6.36 – 7.08 (br, 205H, $-C_6H_5$), 5.11 (m, 1H, −ArCH−), 4.77 (t, J = 7.4 Hz, 2H, $-NCH_2-$), 4.19 (s, 3H, $-NCH_3$), 3.93 (t, J = 6.5 Hz, 2H, $-OCH_2-$), 3.63 (m, 2H, $-CH_2-$) 1.25 – 2.18 (br, 147H, $-CH_2-$, $-CHCH_2-$). $M_{n,NMR}$ = 5000 g mol^{-1}, $M_{n,SEC}$ = 5100 g mol^{-1}, $Đ$ = 1.08.

PS_{53}L-I: Yield: 586 mg, 93%. ^{1}H NMR (400 MHz, $CDCl_3$): δ 8.37 (t, J = 8.0 Hz, 2H, Ar), 8.06 (t, J = 8.0 Hz, 1H, Ar), 7.87 (d, J = 8.0 Hz, 2H, Ar), 7.46 (d, J = 8.0 Hz, 2H, Ar), 7.36 (m, 4H), 6.36 – 7.08 (br, 265H, $-C_6H_5$), 5.11 (m, 1H, −ArCH−), 4.77 (t, J = 7.4 Hz, 2H, $-NCH_2-$), 4.19 (s, 3H, $-NCH_3$), 3.93 (t, J = 6.5 Hz, 2H, $-OCH_2-$), 3.63 (m, 2H, $-CH_2-$) 1.25 – 2.18 (br, 185H, $-CH_2-$, $-CHCH_2-$). $M_{n,NMR}$ = 6300 g mol^{-1}, $M_{n,SEC}$ = 6300 g mol^{-1}, $Đ$ = 1.08.

PS_{73}L-I: Yield: 790 mg, 94%. ^{1}H NMR (400 MHz, $CDCl_3$): δ 8.37 (t, J = 8.0 Hz, 2H, Ar), 8.06 (t, J = 8.0 Hz, 1H, Ar), 7.87 (d, J = 8.0 Hz, 2H, Ar), 7.46 (d, J = 8.0 Hz, 2H, Ar), 7.36 (m, 4H), 6.36 – 7.08 (br, 365H, $-C_6H_5$), 5.11 (m, 1H, −ArCH−), 4.77 (t, J = 7.4 Hz, 2H, $-NCH_2-$), 4.19 (s, 3H, $-NCH_3$), 3.93 (t, J = 6.5 Hz, 2H, $-OCH_2-$), 3.63 (m, 2H, $-CH_2-$) 1.25 – 2.18 (br, 185H, $-CH_2-$, $-CHCH_2-$). $M_{n,NMR}$ = 8400 g mol^{-1}, $M_{n,SEC}$ = 8400 g mol^{-1}, $Đ$ = 1.07.

PS_{14}L-II: Yield: 207 mg, 90%. ^{1}H NMR (400 MHz, $CDCl_3$): δ 7.93 (s, 2H, Ar), 7.88 (d, J = 8.0 Hz, 2H, Ar), 7.46 (d, J = 8.0 Hz, 2H, Ar), 7.36 (m, 4H, Ar), 6.36 – 7.08 (br, 70H, $-C_6H_5$), 5.11 (m, 1H, −ArCH−), 4.24 (s, 8H, $-NCH_3$, $-PyOCH_2-$), 3.97 (t, 2H, J = 6.6 Hz, $-OCH_2-$), 3.63 (m, 2H, $-CH_2-$), 1.25 – 2.18 (br, 63H, $-CH_2-$, $-CHCH_2-$). $M_{n,NMR}$ = 2300 g mol^{-1}, $M_{n,SEC}$ = 2100 g mol^{-1}, $Đ$ = 1.11.

PS_{19}L-II: Yield: 252 mg, 90%. ^{1}H NMR (400 MHz, $CDCl_3$): δ 7.93 (s, 2H, Ar), 7.88 (d, J = 8.0 Hz, 2H, Ar), 7.46 (d, J = 8.0 Hz, 2H, Ar), 7.36 (m, 4H, Ar), 6.36 – 7.08 (br, 95H, $-C_6H_5$), 5.11 (m, 1H, −ArCH−), 4.24 (s, 8H, $-NCH_3$, $-PyOCH_2-$), 3.97 (t, 2H, J = 6.6 Hz, $-OCH_2-$), 3.63 (m, 2H, $-CH_2-$), 1.25 – 2.18 (br, 78H, $-CH_2-$, $-CHCH_2-$). $M_{n,NMR}$ = 2800 g mol^{-1}, $M_{n,SEC}$ = 2600 g mol^{-1}, $Đ$ = 1.07.

PS_{24}L-II: Yield: 303 mg, 92%. ^{1}H NMR (400 MHz, $CDCl_3$): δ 7.93 (s, 2H, Ar), 7.88 (d, J = 8.0 Hz, 2H, Ar), 7.46 (d, J = 8.0 Hz, 2H, Ar), 7.36 (m, 4H, Ar), 6.36 – 7.08 (br, 120H, $-C_6H_5$), 5.11 (m, 1H, −ArCH−), 4.24 (s, 8H, $-NCH_3$, $-PyOCH_2-$), 3.97 (t, 2H, J = 6.6 Hz, $-OCH_2-$), 3.63 (m, 2H, $-CH_2-$), 1.25 – 2.18 (br, 94H, $-CH_2-$, $-CHCH_2-$). $M_{n,NMR}$ = 3300 g mol^{-1}, $M_{n,SEC}$ = 3100 g mol^{-1}, $Đ$ = 1.08.

PS$_{34}$L-II: Yield: 400 mg, 93%. ^{1}H NMR (400 MHz, CDCl$_3$): δ 7.93 (s, 2H, Ar), 7.88 (d, J = 8.0 Hz, 2H, Ar), 7.46 (d, J = 8.0 Hz, 2H, Ar), 7.36 (m, 4H, Ar), 6.36 – 7.08 (br, 170H, −C$_6$H$_5$), 5.11 (m, 1H, −ArCH−), 4.24 (s, 8H, −NCH$_3$, −PyOCH$_2$−), 3.97 (t, 2H, J = 6.6 Hz, −OCH$_2$−), 3.63 (m, 2H, −CH$_2$−), 1.25 – 2.18 (br, 123H, −CH$_2$−, −CHCH$_2$−). $M_{n,NMR}$ = 4400 g mol^{-1}, $M_{n,SEC}$ = 4500 g mol^{-1}, $Đ$ = 1.07.

PS$_{41}$L-II: Yield: 470 mg, 92%. ^{1}H NMR (400 MHz, CDCl$_3$): δ 7.93 (s, 2H, Ar), 7.88 (d, J = 8.0 Hz, 2H, Ar), 7.46 (d, J = 8.0 Hz, 2H, Ar), 7.36 (m, 4H, Ar), 6.36 – 7.08 (br, 205H, −C$_6$H$_5$), 5.11 (m, 1H, −ArCH−), 4.24 (s, 8H, −NCH$_3$, −PyOCH$_2$−), 3.97 (t, 2H, J = 6.6 Hz, −OCH$_2$−), 3.63 (m, 2H, −CH$_2$−), 1.25 – 2.18 (br, 145H, −CH$_2$−, −CHCH$_2$−). $M_{n,NMR}$ = 5100 g mol^{-1}, $M_{n,SEC}$ = 5300 g mol^{-1}, $Đ$ = 1.08.

PS$_{53}$L-II: Yield: 584 mg, 93%. ^{1}H NMR (400 MHz, CDCl$_3$): δ 7.93 (s, 2H, Ar), 7.88 (d, J = 8.0 Hz, 2H, Ar), 7.46 (d, J = 8.0 Hz, 2H, Ar), 7.36 (m, 4H, Ar), 6.36 – 7.08 (br, 265H, −C$_6$H$_5$), 5.11 (m, 1H, −ArCH−), 4.24 (s, 8H, −NCH$_3$, −PyOCH$_2$−), 3.97 (t, 2H, J = 6.6 Hz, −OCH$_2$−), 3.63 (m, 2H, −CH$_2$−), 1.25 – 2.18 (br, 180H, −CH$_2$−, −CHCH$_2$−). $M_{n,NMR}$ = 6300 g mol^{-1}, $M_{n,SEC}$ = 6200 g mol^{-1}, $Đ$ = 1.08.

PS$_{73}$L-II: Yield: 781 mg, 93%. ^{1}H NMR (400 MHz, CDCl$_3$): δ 7.93 (s, 2H, Ar), 7.88 (d, J = 8.0 Hz, 2H, Ar), 7.46 (d, J = 8.0 Hz, 2H, Ar), 7.36 (m, 4H, Ar), 6.36 – 7.08 (br, 365H, −C$_6$H$_5$), 5.11 (m, 1H, −ArCH−), 4.24 (s, 8H, −NCH$_3$, −PyOCH$_2$−), 3.97 (t, 2H, J = 6.6 Hz, −OCH$_2$−), 3.63 (m, 2H, −CH$_2$−), 1.25 – 2.18 (br, 240H, −CH$_2$−, −CHCH$_2$−). $M_{n,NMR}$ = 8400 g mol^{-1}, $M_{n,SEC}$ = 8600 g mol^{-1}, $Đ$ = 1.05.

Table S1 Molecular characteristics of PS$_n$-Br (n = 14, 19, 24, 34, 41, 53, 73)

Sample	M_n [a]	$Đ$ [a]	Sample	M_n [a]	$Đ$ [a]
PS$_{14}$-Br	1500	1.06	PS$_{41}$-Br	4300	1.07
PS$_{19}$-Br	2000	1.08	PS$_{53}$-Br	5600	1.09
PS$_{24}$-Br	2600	1.08	PS$_{73}$-Br	7600	1.07
PS$_{34}$-Br	3500	1.10			

[a] The values of M_n and $Đ$ were obtained from SEC measurements.

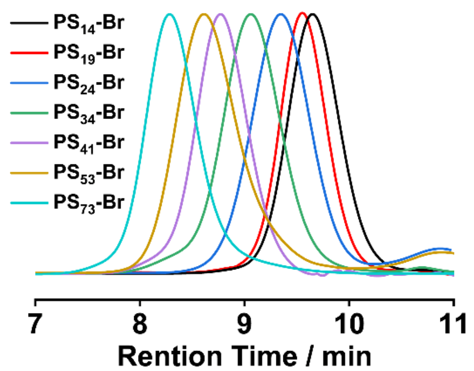

Fig. S1 SEC traces of PS$_n$-Br (n = 14, 19, 24, 34, 41, 53, 73).

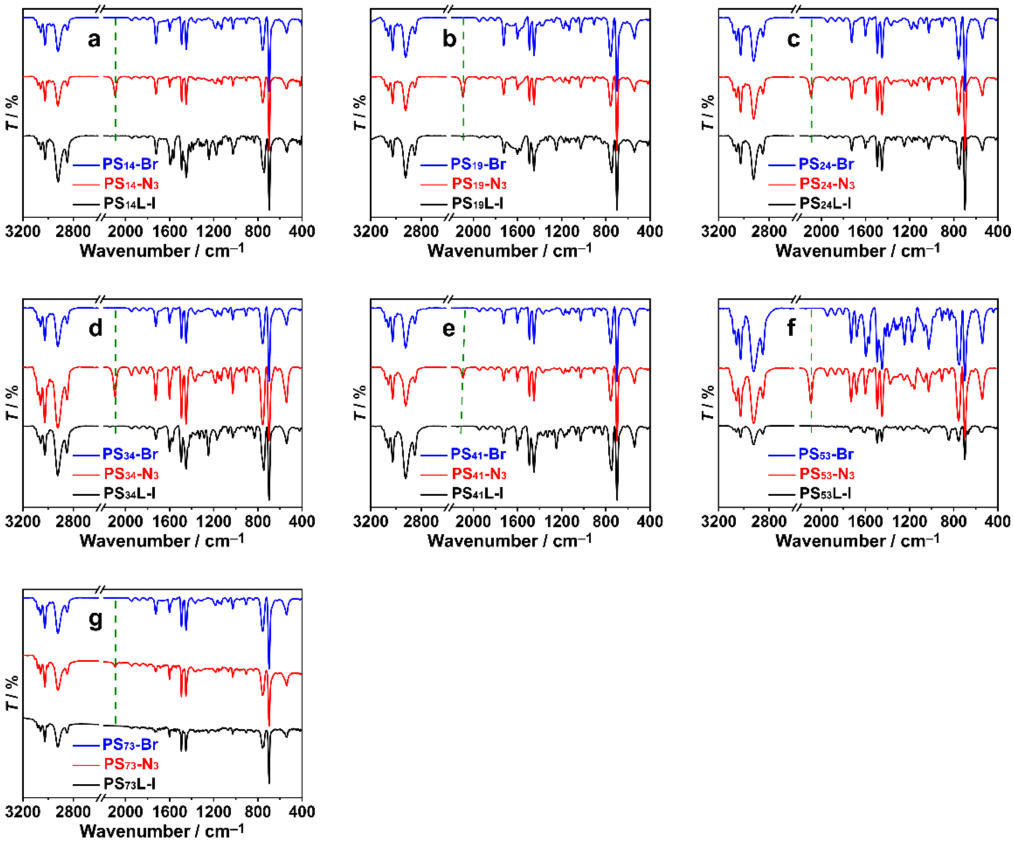

Fig. S2 FT-IR spectra of PS$_n$L-Br, PS$_n$-N$_3$, and **PS$_n$L-I** (n = 14, 19, 24, 34, 41, 53, 73).

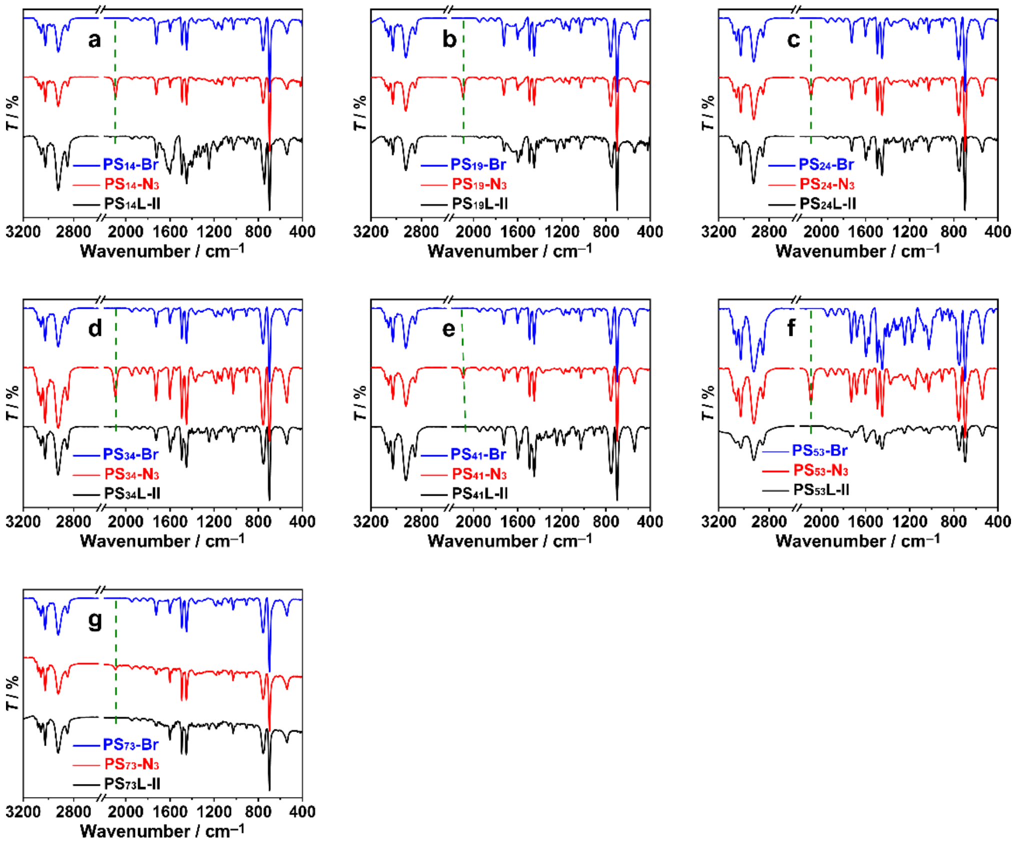

Fig. S3 FT-IR spectra of PS$_n$-Br, PS$_n$-N$_3$, and **PS$_n$L-II** (n = 14, 19, 24, 34, 41, 53, 73).

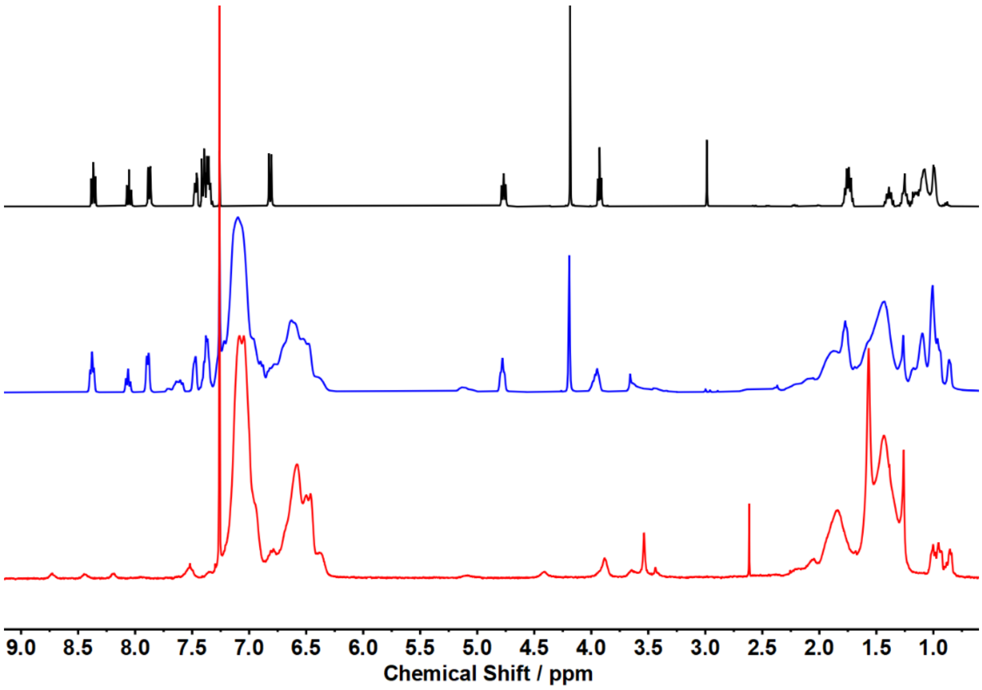

Fig. S4 [1]H NMR spectra of **L-I** (Top), **PS$_{19}$L-I** (Center), and **PS$_{19}$Pt-I** (Bottom) in $CDCl_3$.

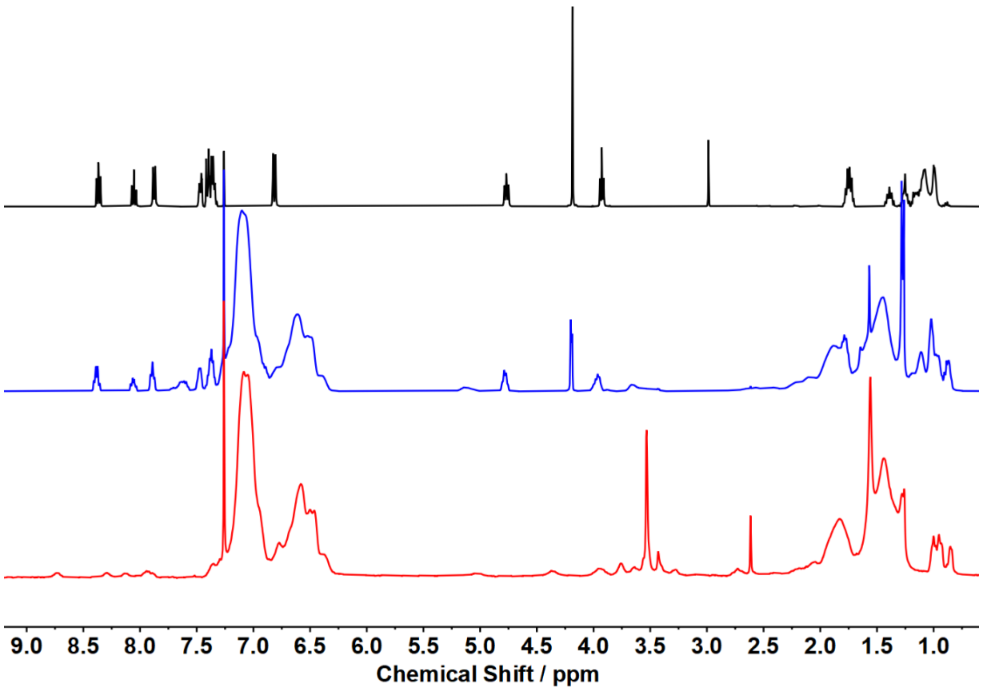

Fig. S5 [1]H NMR spectra of **L-I** (Top), **PS$_{24}$L-I** (Center), and **PS$_{24}$Pt-I** (Bottom) in $CDCl_3$.

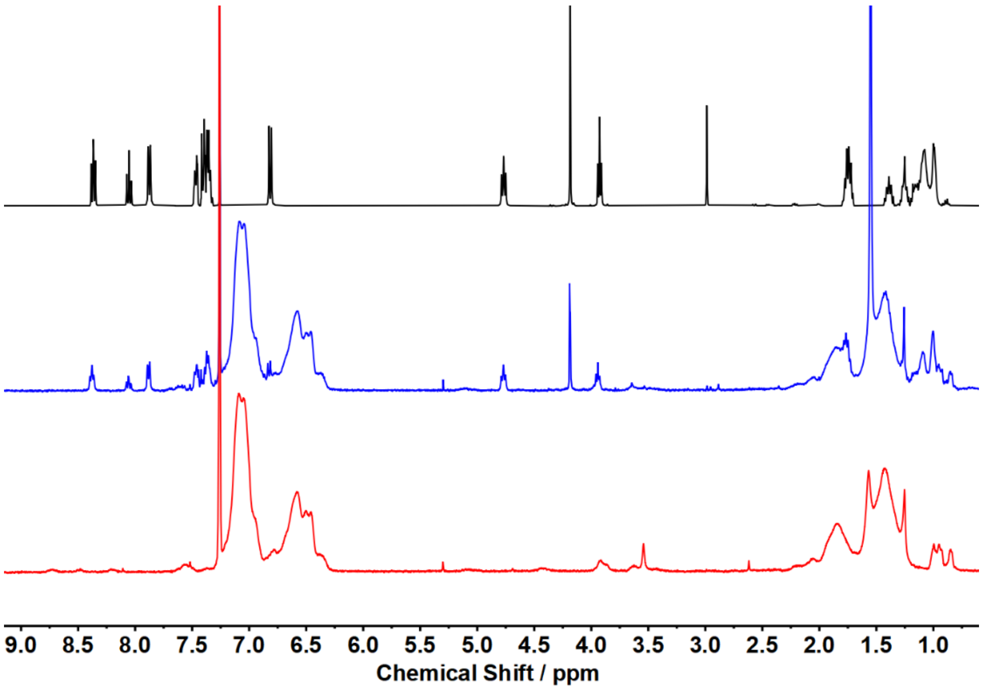

Fig. S6 [1]H NMR spectra of **L-I** (Top), **PS$_{34}$L-I** (Center), and **PS$_{34}$Pt-I** (Bottom) in $CDCl_3$.

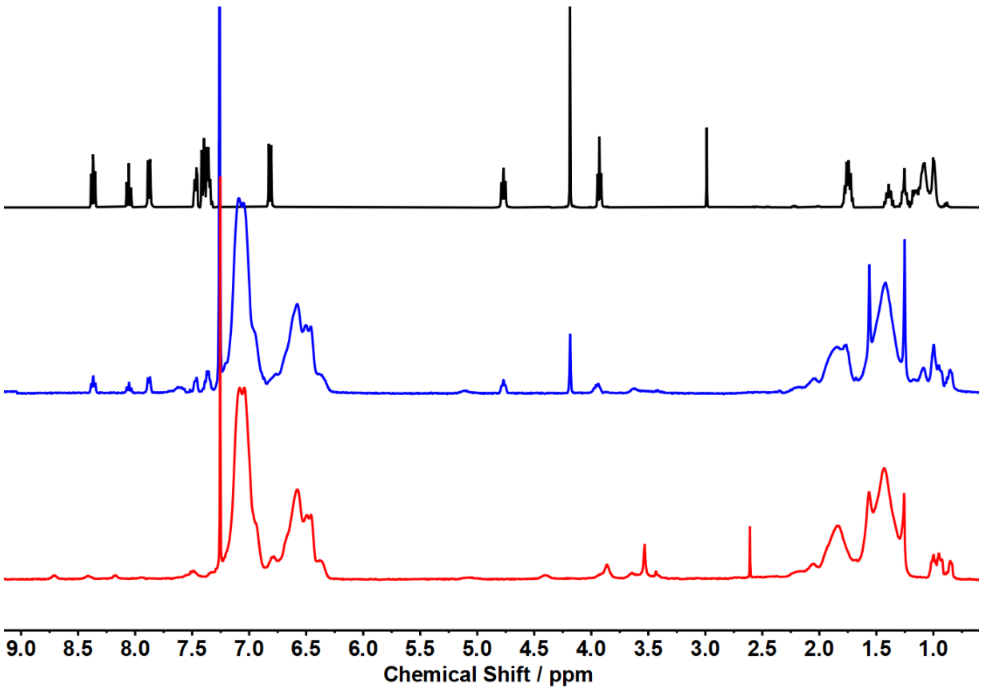

Fig. S7 [1]H NMR spectra of **L-I** (Top), **PS$_{41}$L-I** (Center), and **PS$_{41}$Pt-I** (Bottom) in $CDCl_3$.

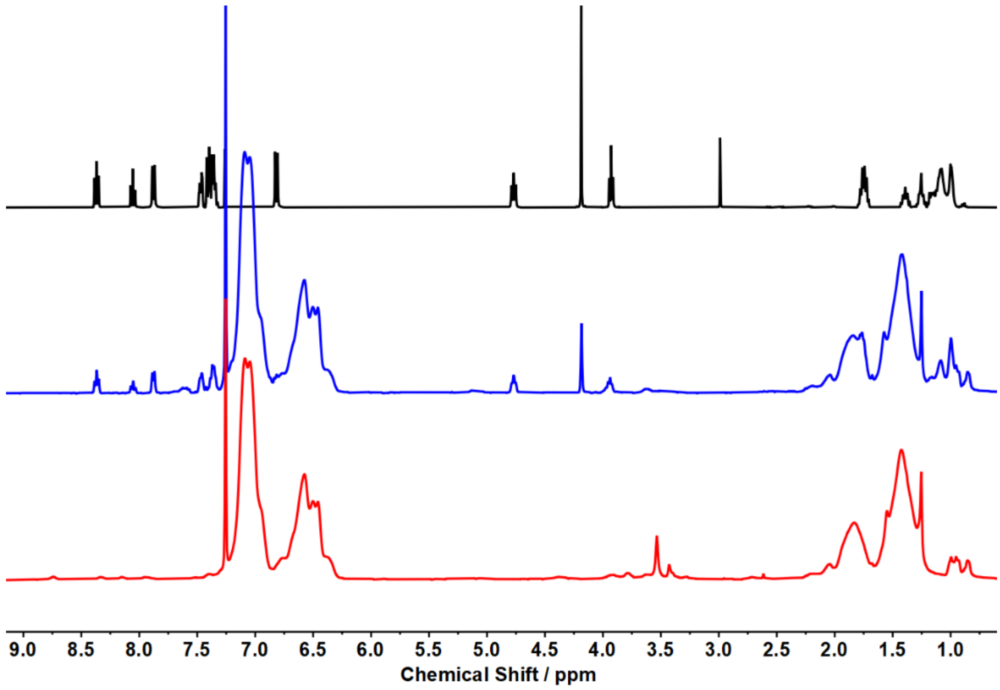

Fig. S8 [1]H NMR spectra of **L-I** (Top), **PS$_{53}$L-I** (Center), and **PS$_{53}$Pt-I** (Bottom) in $CDCl_3$.

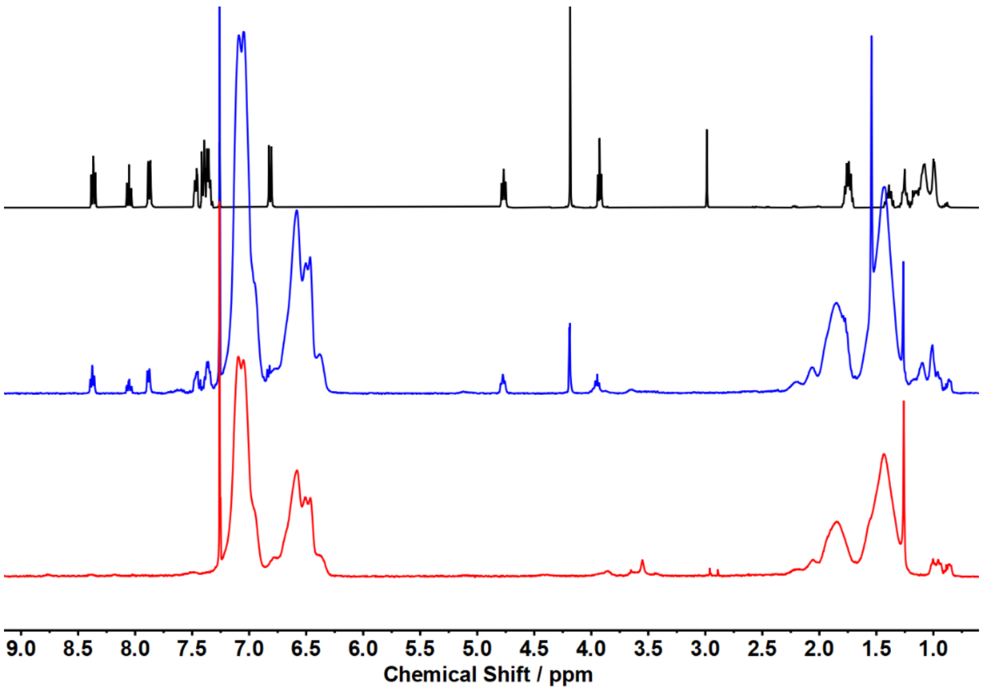

Fig. S9 [1]H NMR spectra of **L-I** (Top), **PS$_{73}$L-I** (Center), and **PS$_{73}$Pt-I** (Bottom) in $CDCl_3$.

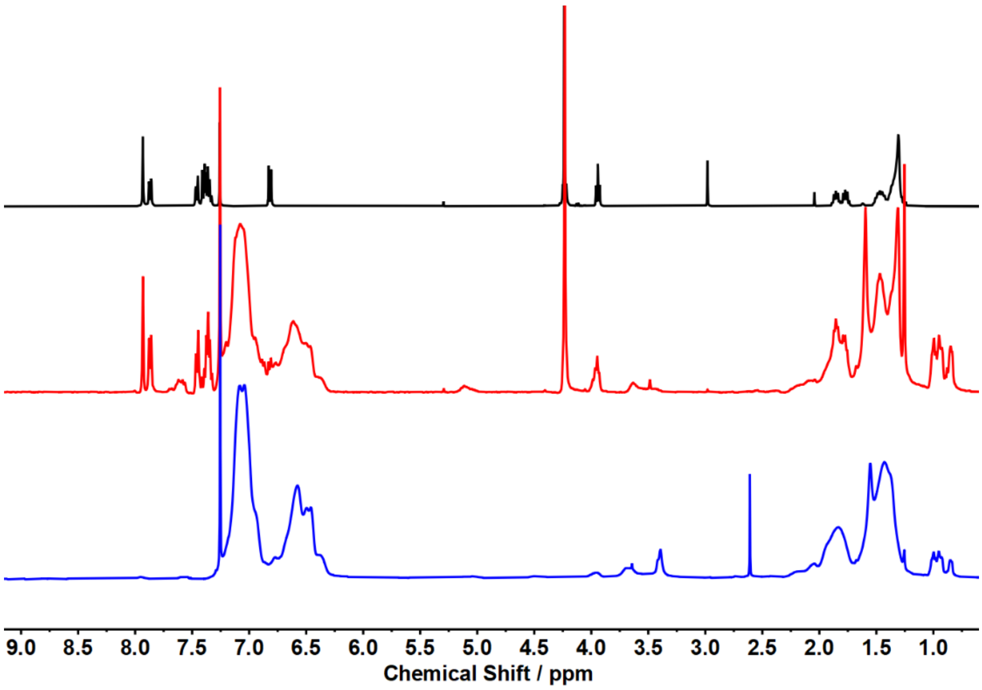

Fig. S10 [1]H NMR spectra of **L-II** (Top), **PS$_{14}$L-II** (Center), and **PS$_{14}$Pt-II** (Bottom) in $CDCl_3$.

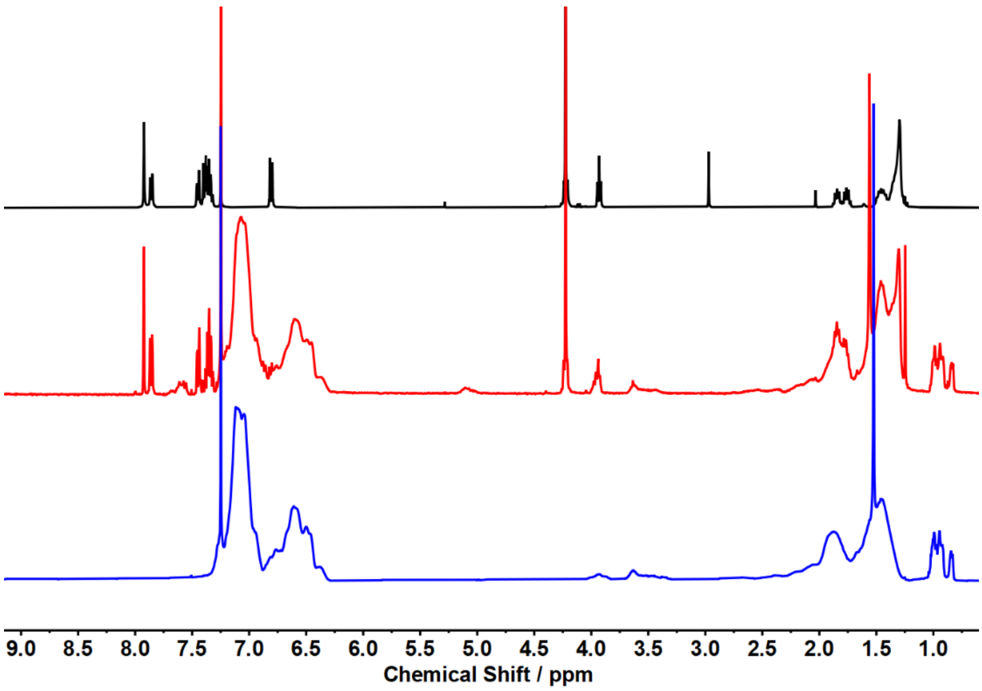

Fig. S11 [1]H NMR spectra of **L-II** (Top), **PS$_{19}$L-II** (Center), and **PS$_{19}$Pt-II** (Bottom) in $CDCl_3$.

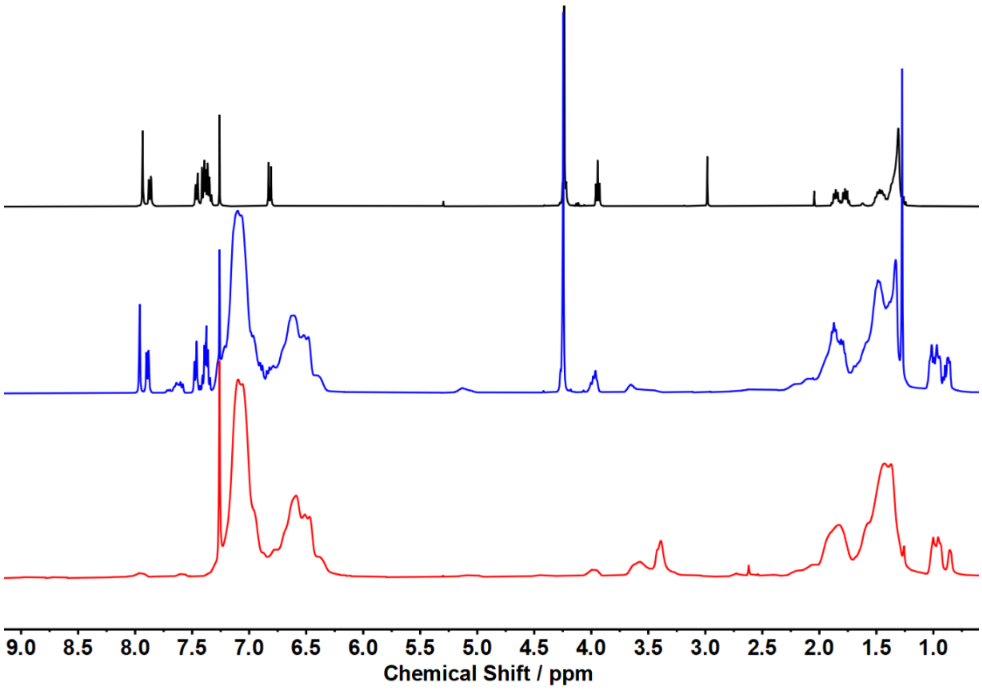

Fig. S12 [1]H NMR spectra of **L-II** (Top), **PS$_{24}$L-II** (Center), and **PS$_{24}$Pt-II** (Bottom) in $CDCl_3$.

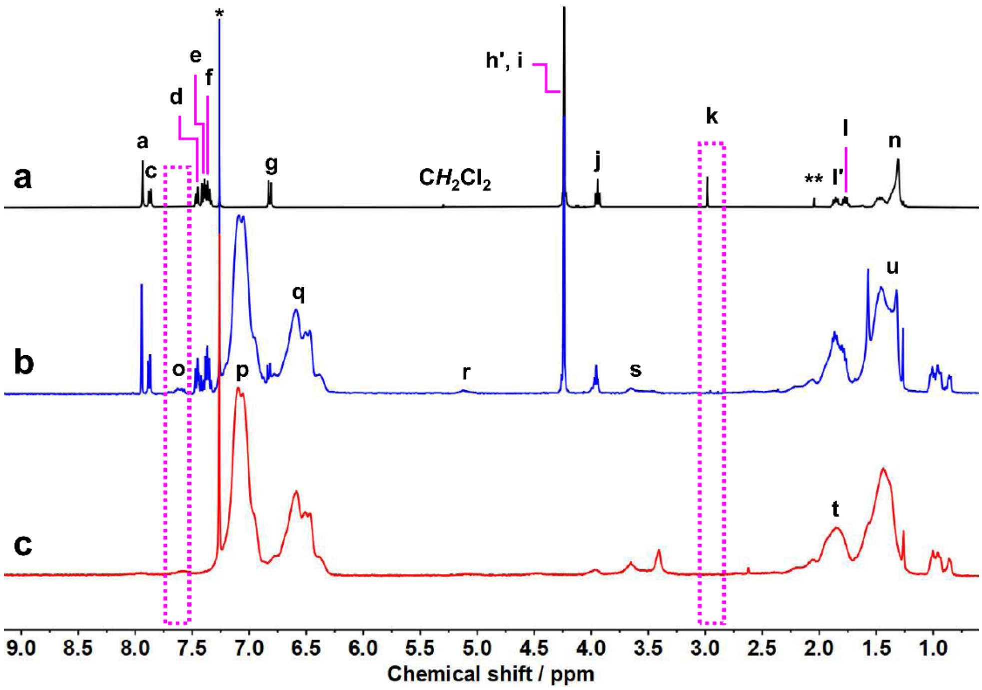

Fig. S13 [1]H NMR spectra of **L-II** (Top), **PS$_{34}$L-II** (Center), and **PS$_{34}$Pt-II** (Bottom) in $CDCl_3$.

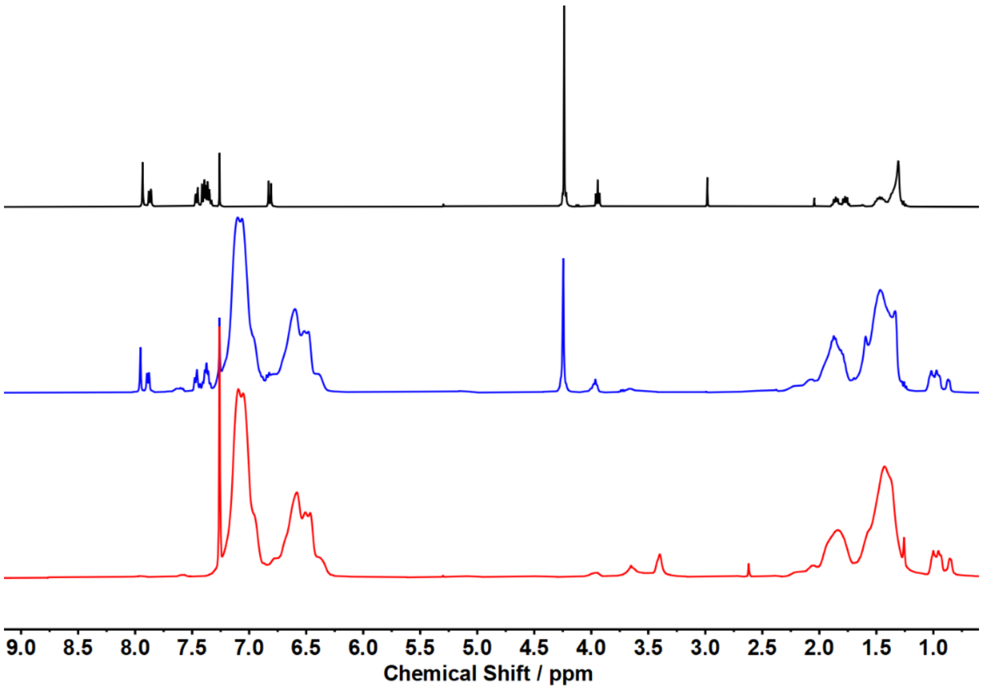

Fig. S14 ^{1}H NMR spectra of **L-II** (Top), **PS$_{41}$L-II** (Center), and **PS$_{41}$Pt-II** (Bottom) in $CDCl_3$.

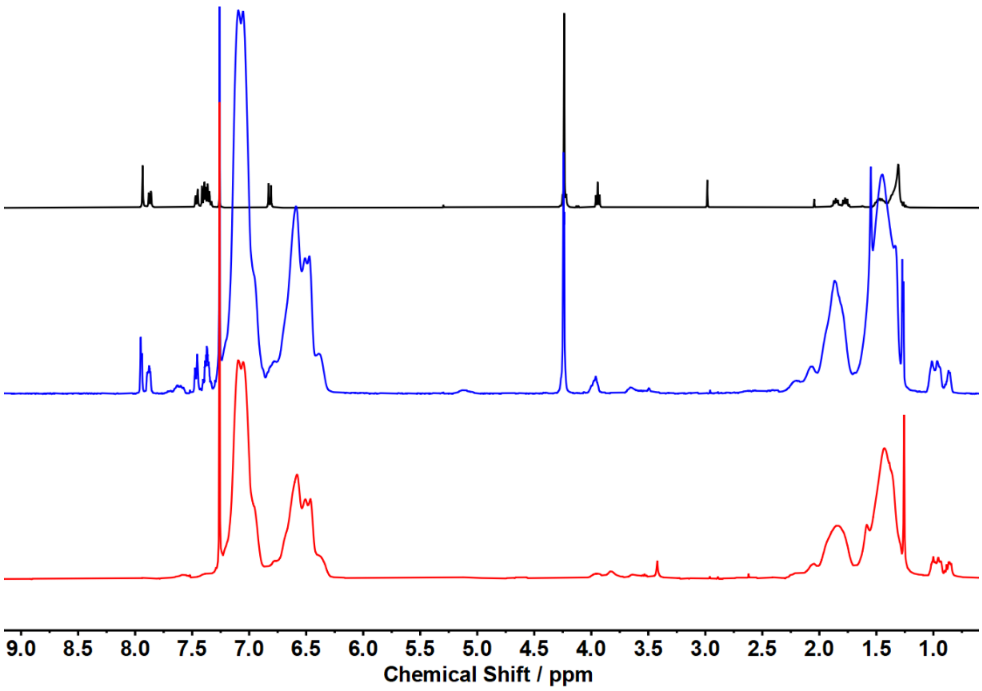

Fig. S15 ^{1}H NMR spectra of **L-II** (Top), **PS$_{53}$L-II** (Center), and **PS$_{53}$Pt-II** (Bottom) in $CDCl_3$.

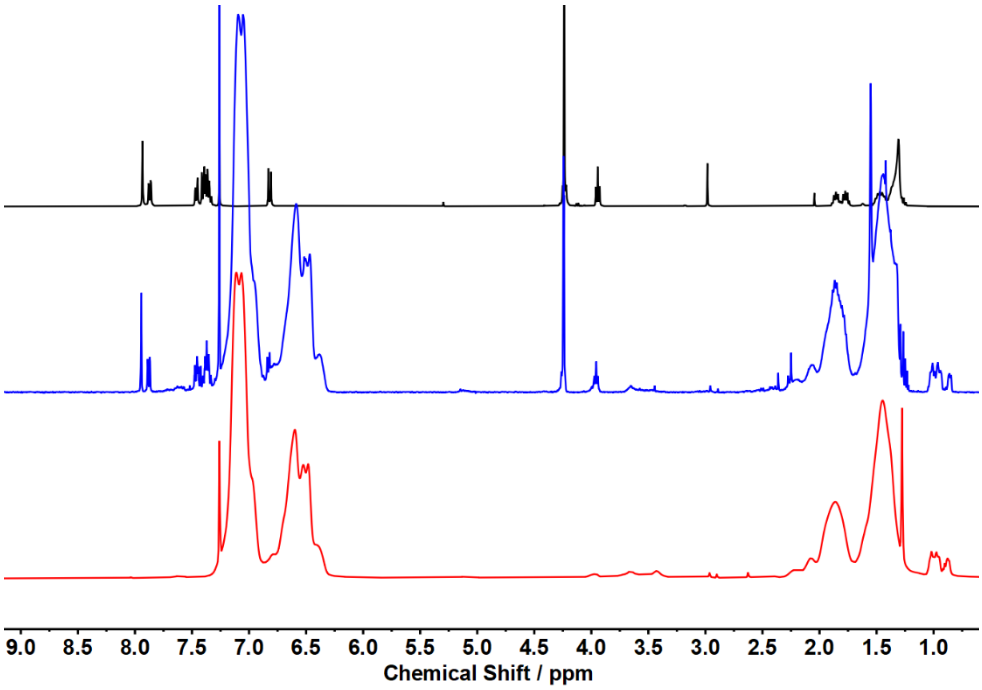

Fig. S16 [1]H NMR spectra of **L-II** (Top), **PS$_{73}$L-II** (Center), and **PS$_{73}$Pt-II** (Bottom) in $CDCl_3$.

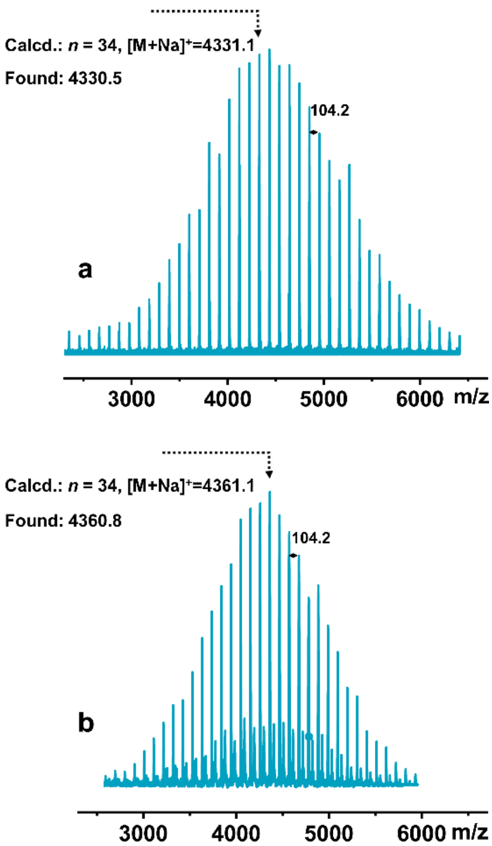

Fig. S17 MALDI-TOF mass spectra of **PS$_{34}$L-I** (a) and **PS$_{34}$L-II** (b).

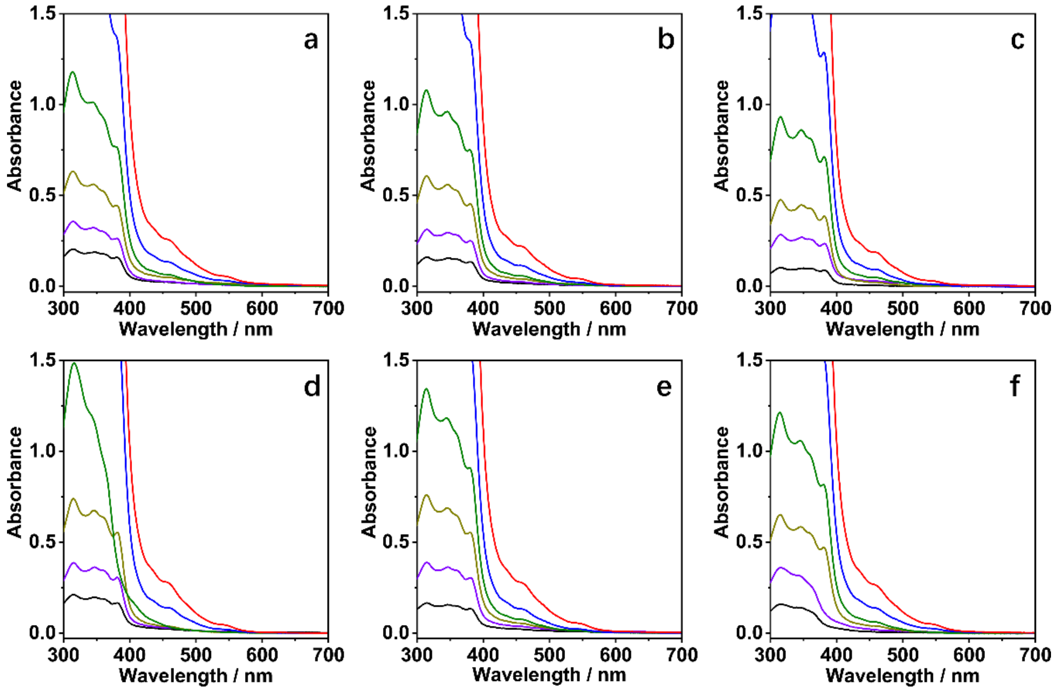

Fig. S18 UV-vis absorption of **PS$_{14}$Pt-I** (a), **PS$_{24}$Pt-I** (b), **PS$_{34}$Pt-I** (c), **PS$_{41}$Pt-I** (d), **PS$_{53}$Pt-I** (e), and **PS$_{73}$Pt-I** (f) in chloroform with increasing concentration (6.25×10^{-6}, 1.25×10^{-5}, 2.5×10^{-5}, 5.0×10^{-5}, 1.0×10^{-4}, and 2×10^{-4} mol L^{-1}).

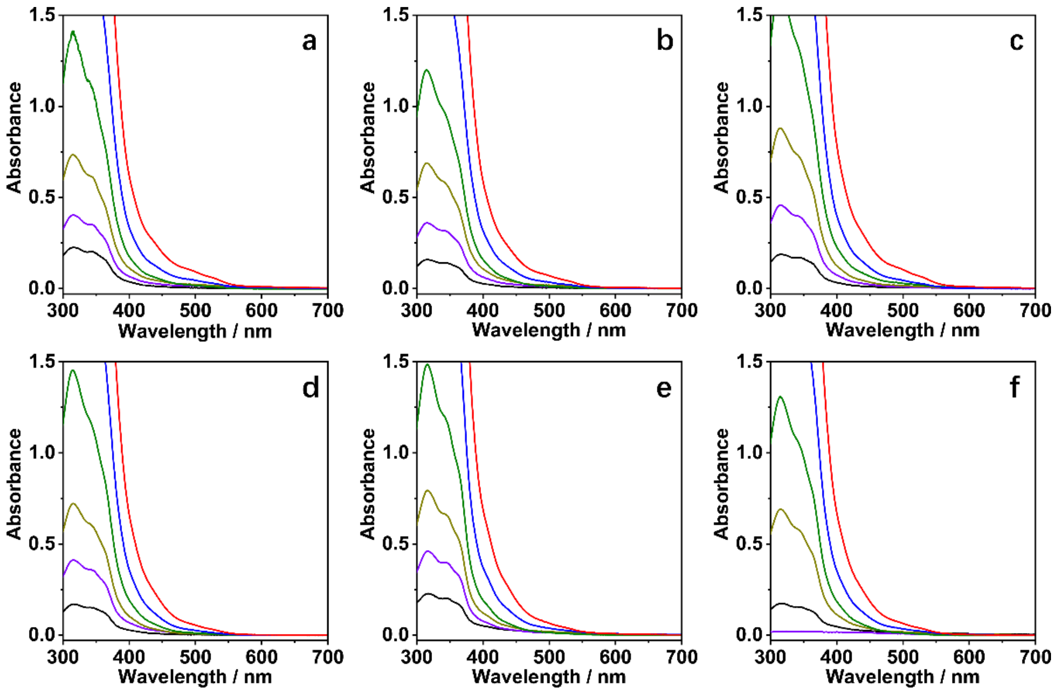

Fig. S19 UV-vis absorption of **PS$_{14}$Pt-II** (a), **PS$_{19}$Pt-II** (b), **PS$_{24}$Pt-II** (c), **PS$_{34}$Pt-II** (d), **PS$_{53}$Pt-II** (e), and **PS$_{73}$Pt-I** (f) in chloroform with the increasing concentration (6.25×10^{-6}, 1.25×10^{-5}, 2.5×10^{-5}, 5.0×10^{-5}, 1.0×10^{-4}, and 2×10^{-4} mol L^{-1}).

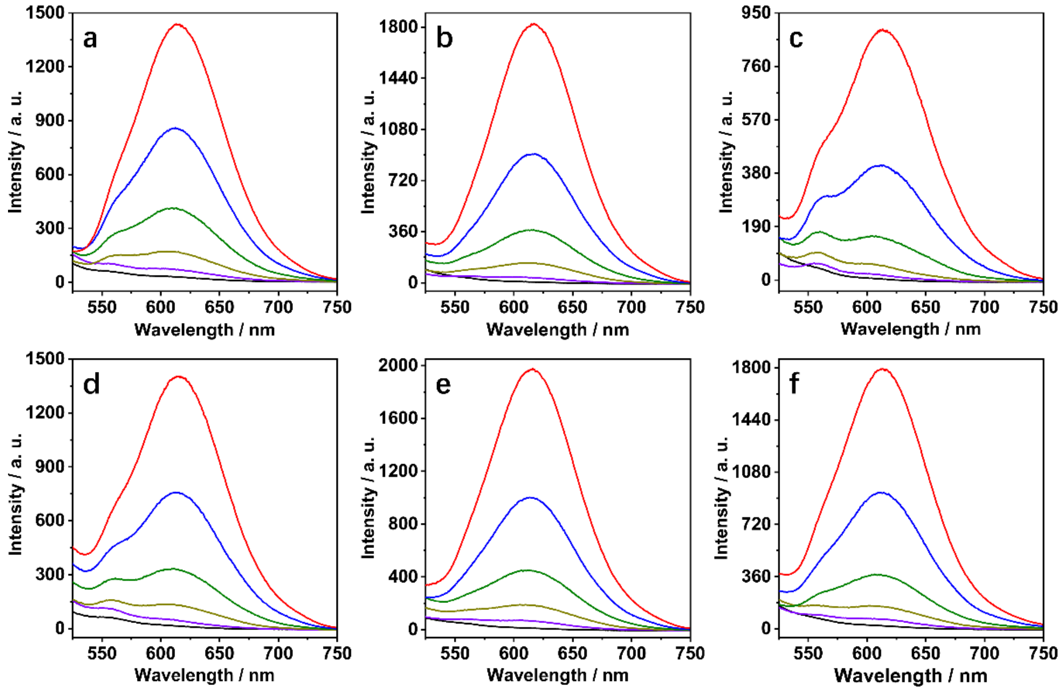

Fig. S20 Luminescence spectra of **PS_{14}Pt-I** (a), **PS_{24}Pt-I** (b), **PS_{34}Pt-I** (c), **PS_{41}Pt-I** (d), **PS_{53}Pt-I** (e), and **PS_{73}Pt-I** (f) in chloroform with the increasing concentration (6.25×10^{-6}, 1.25×10^{-5}, 2.5×10^{-5}, 5.0×10^{-5}, 1.0×10^{-4}, and 2×10^{-4} mol L^{-1}).

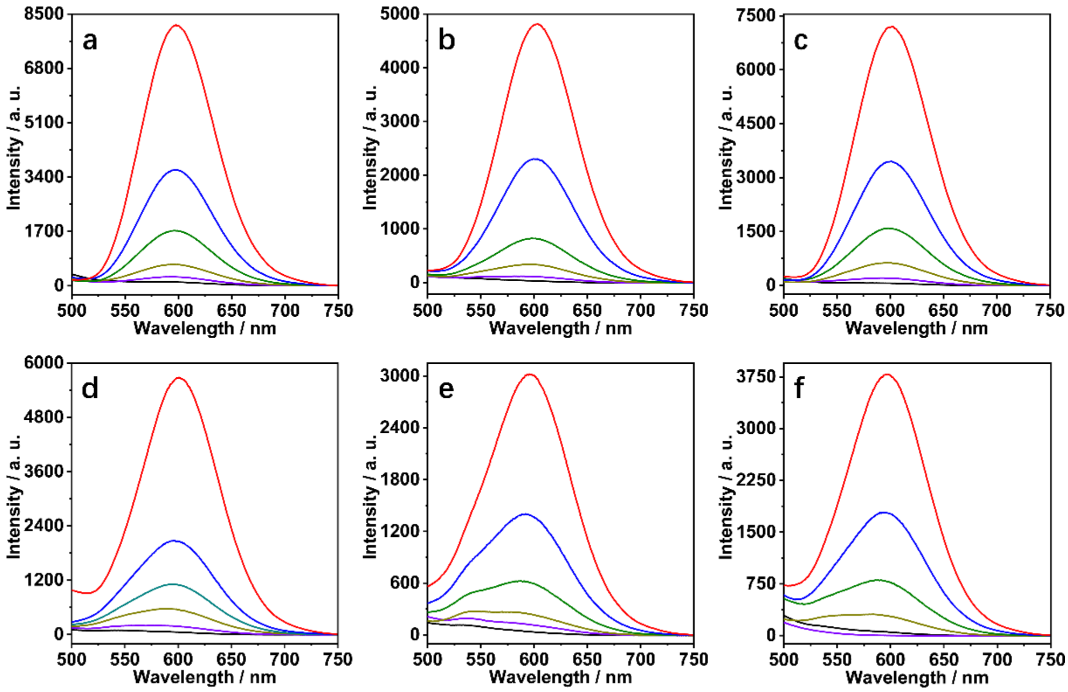

Fig. S21 Luminescence spectra of **PS_{14}Pt-II** (a), **PS_{19}Pt-II** (b), **PS_{24}Pt-II** (c), **PS_{34}Pt-II** (d), **PS_{53}Pt-II** (e), and **PS_{73}Pt-II** (f) in chloroform with the increasing concentration (6.25×10^{-6}, 1.25×10^{-5}, 2.5×10^{-5}, 5.0×10^{-5}, 1.0×10^{-4}, and 2×10^{-4} mol L^{-1}).

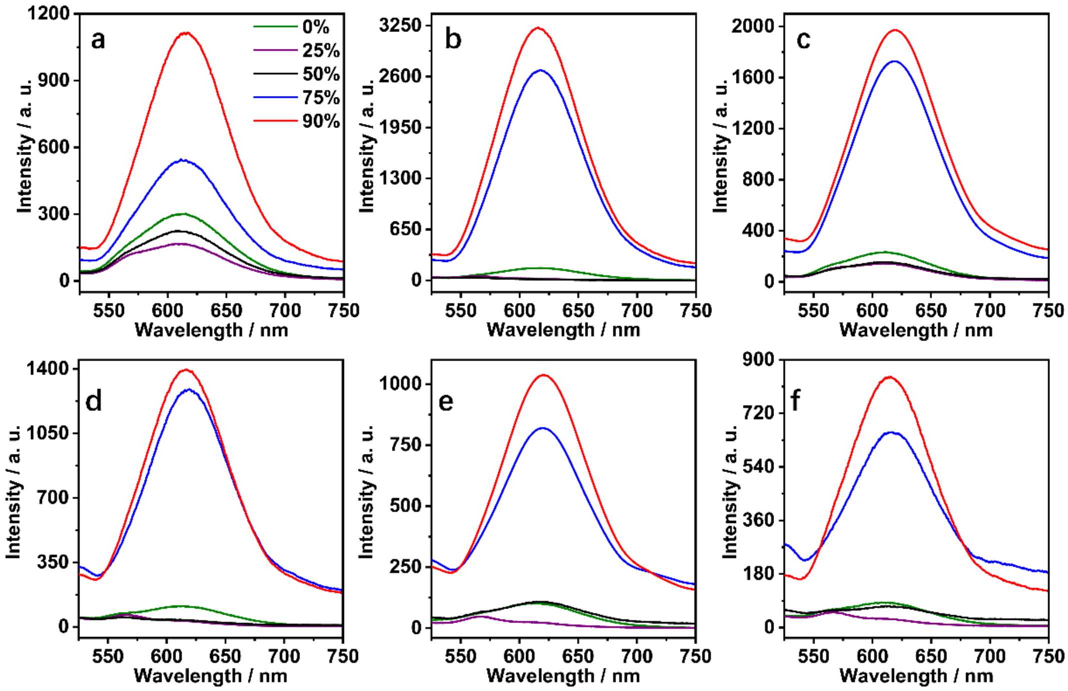

Fig. S22 Luminescence spectra of **PS_{14}Pt-I** (a), **PS_{24}Pt-I** (b), **PS_{34}Pt-I** (c), **PS_{41}Pt-I** (d), **PS_{53}Pt-I** (e), and **PS_{73}Pt-I** (f) with increasing methanol content in chloroform.

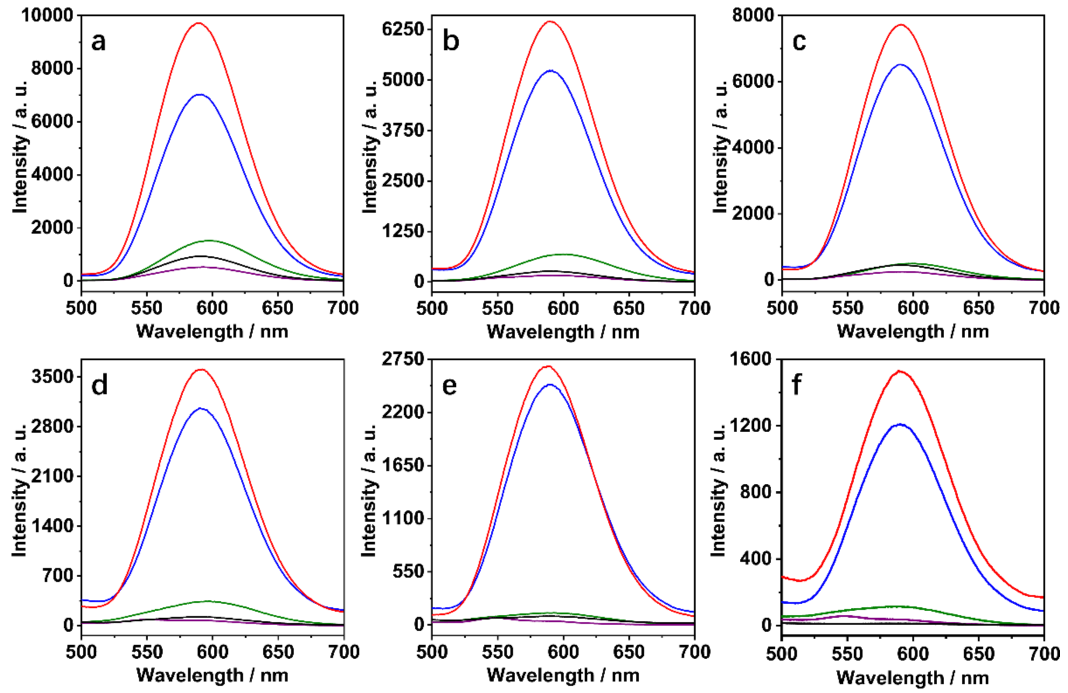

Fig. S23 Luminescence spectra of **PS_{14}Pt-II** (a), **PS_{19}Pt-II** (b), **PS_{24}Pt-II** (c), **PS_{34}Pt-II** (d), **PS_{53}Pt-II** (e), and **PS_{73}Pt-II** (f) with increasing methanol content in chloroform.

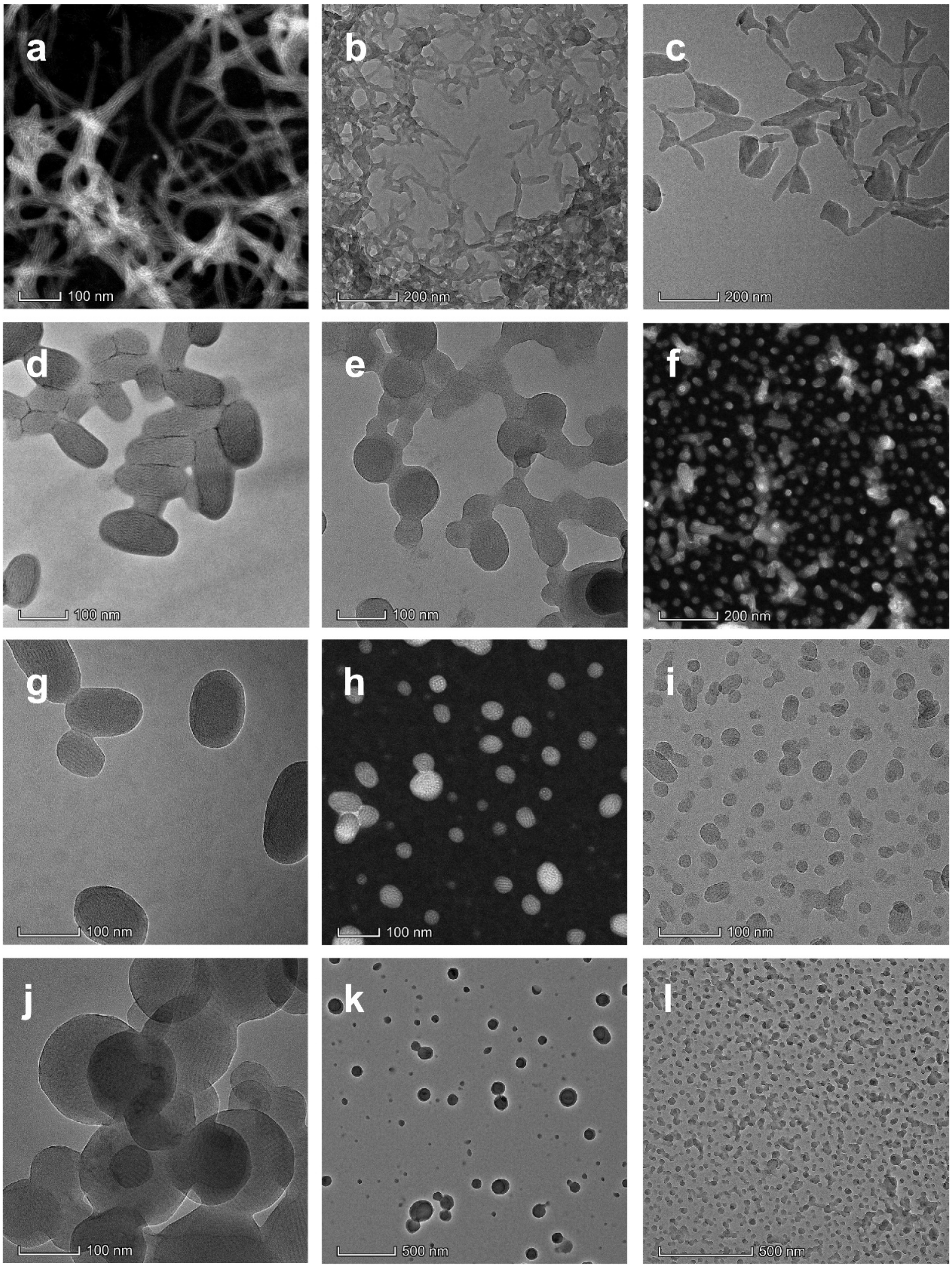
a
100 nm
b
200 nm
c
200 nm
d
100 nm
e
100 nm
f
200 nm
g
100 nm
h
100 nm
i
100 nm
j
100 nm
k
500 nm
l
500 nm

Fig. S24 Continued

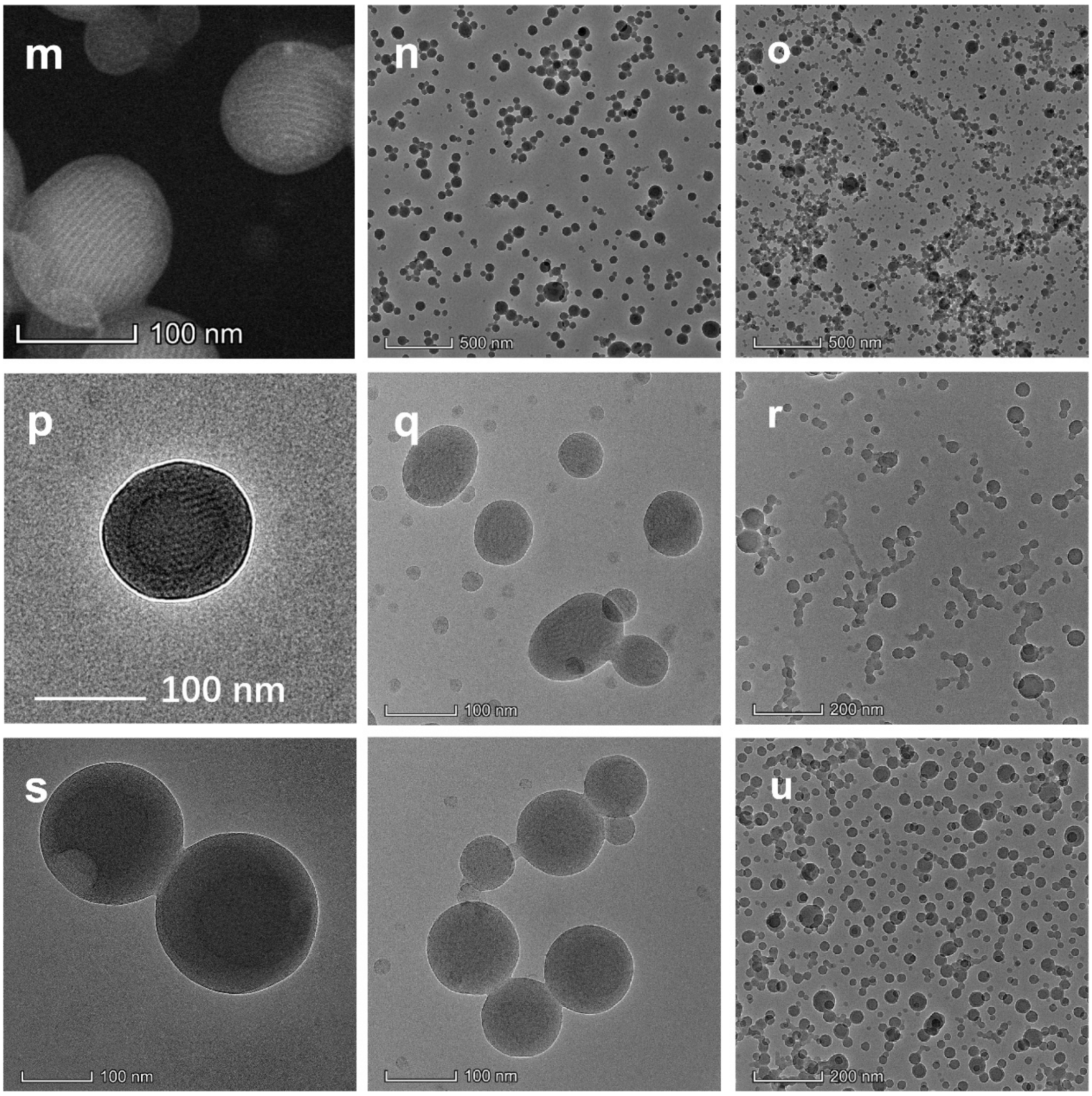

Fig. S24 TEM images of **PS_{14}Pt-I** (a, b, c), **PS_{19}Pt-I** (d, e, f), **PS_{24}Pt-I** (g, h, i), **PS_{34}Pt-I** (j, k, l) in **PS_{41}Pt-I** (m, n, o), **PS_{53}Pt-I** (p, q, r), **PS_{73}Pt-I** (s, t, u) in chloroform/methanol mixture solvent with methanol contents of 50 vol%, 75 vol%, and 90 vol%.

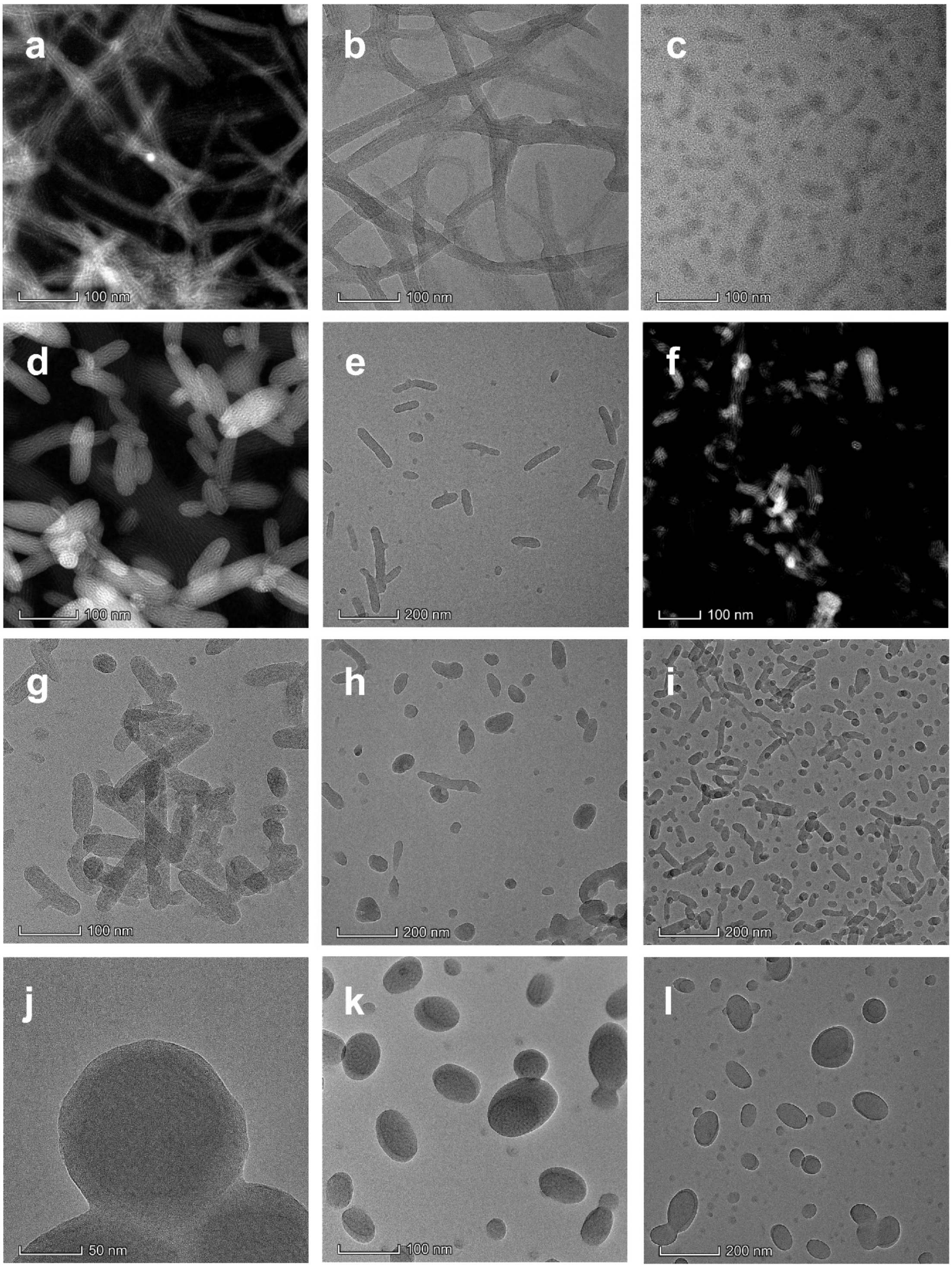
a
100 nm
b
100 nm
c
100 nm
d
100 nm
e
200 nm
f
100 nm
g
100 nm
h
200 nm
i
200 nm
j
50 nm
k
100 nm
l
200 nm

Fig. S25 Continued

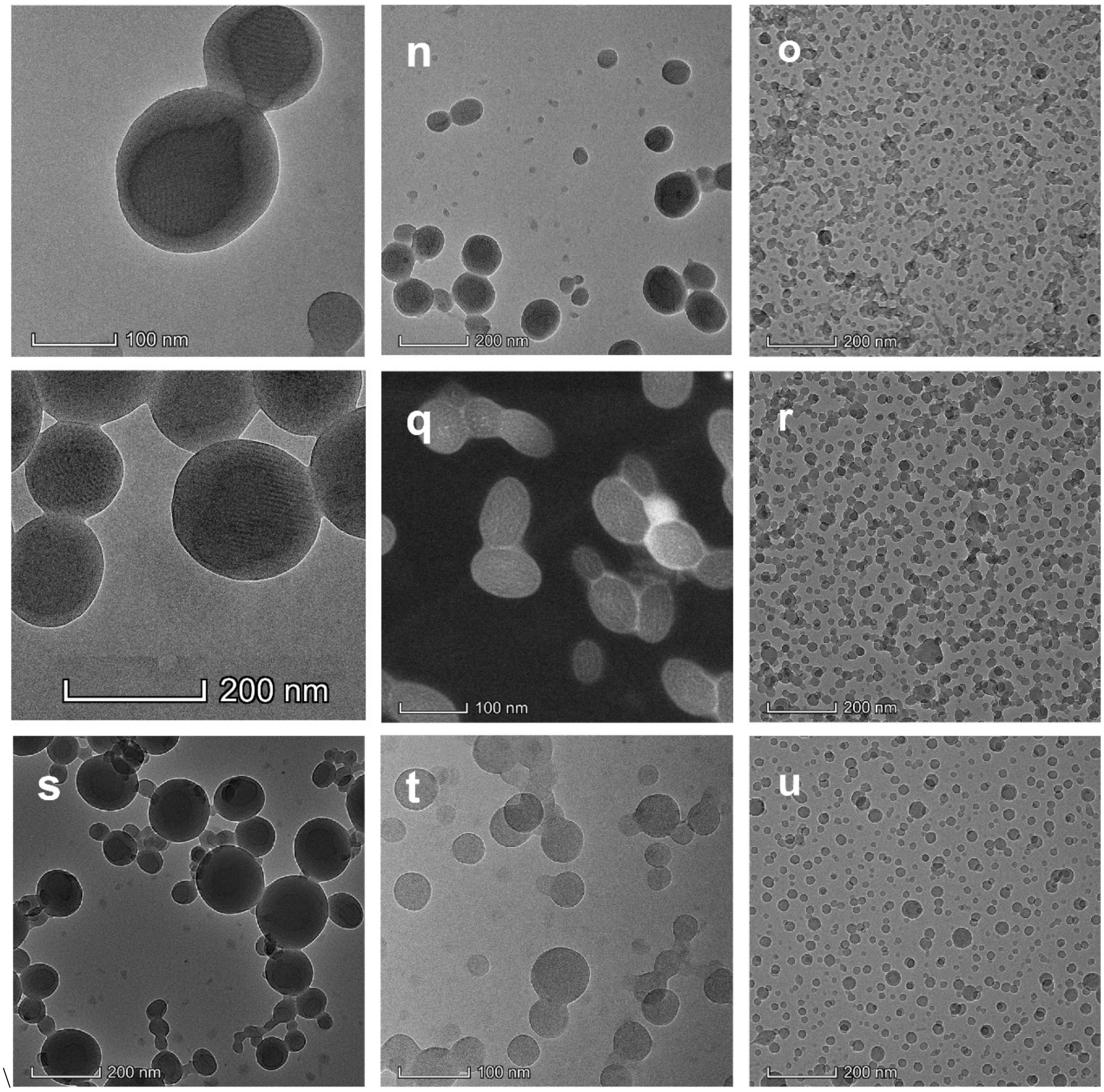

Fig. S25 TEM images of **PS$_{14}$Pt-II** (a, b, c), **PS$_{19}$Pt-II** (d, e, f), **PS$_{24}$Pt-II** (g, h, i), **PS$_{34}$Pt-II** (j, k, l), **PS$_{41}$Pt-II** (m, n, o), **PS$_{53}$Pt-II** (p, q, r), **PS$_{73}$Pt-II** (s, t, u) in chloroform/methanol mixture solvent with methanol contents of 50 vol%, 75 vol%, and 90 vol%.

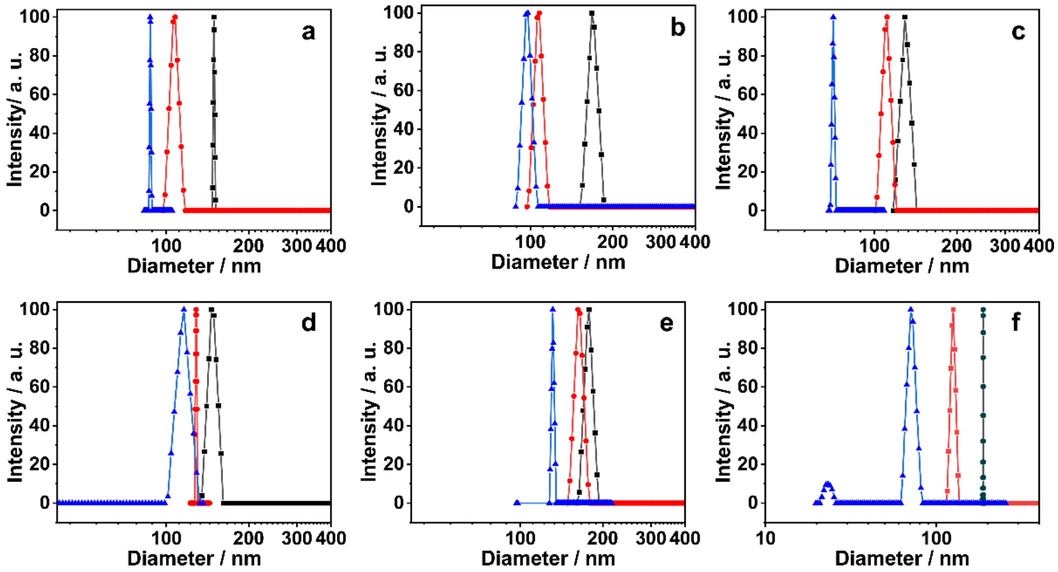

Fig. S26 DLS overlay of **PS_{14}Pt-I** (a), **PS_{19}Pt-I** (b), **PS_{24}Pt-I** (c) **PS_{34}Pt-I** (d) **PS_{41}Pt-I** (e) and **PS_{73}Pt-I** (f) in chloroform/methanol mixture solvent with methanol contents of 50 vol% (black), 75 vol% (red), and 90 vol%(blue).

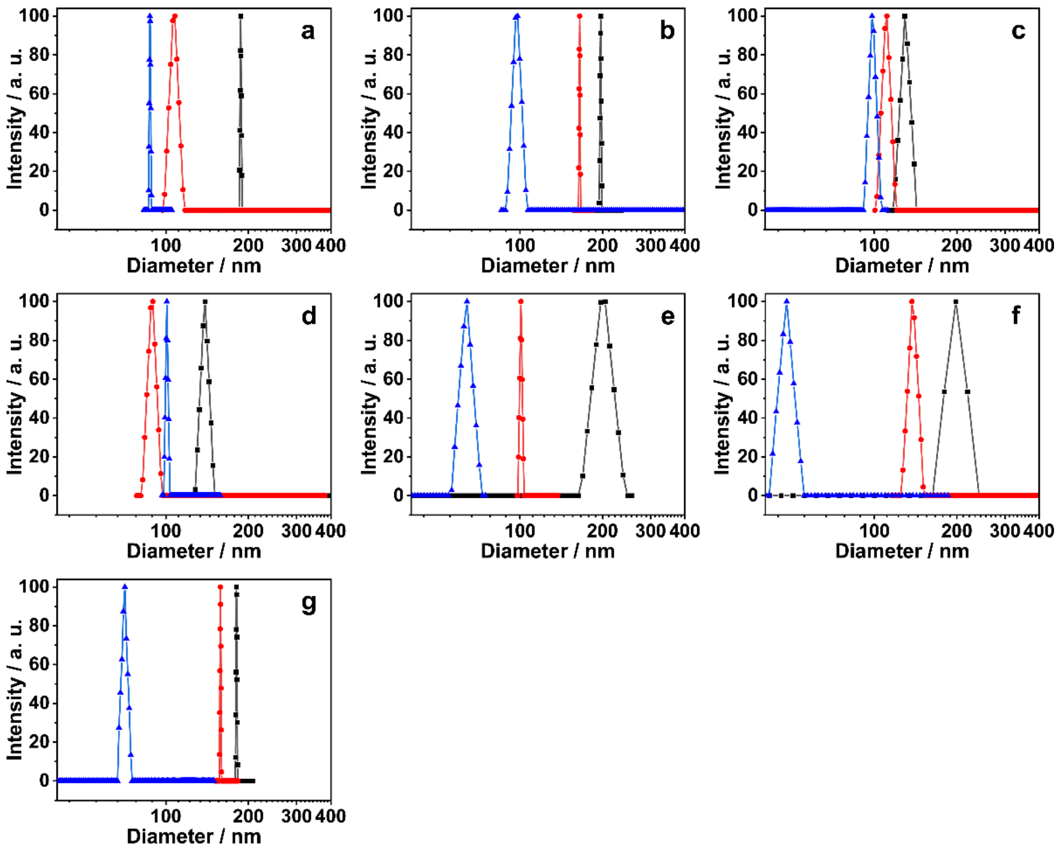

Fig. S27 DLS overlay of **PS_{14}Pt-II** (a), **PS_{19}Pt-II** (b), **PS_{24}Pt-II** (c) **PS_{34}Pt-II** (d) **PS_{41}Pt-II** (e) **PS_{53}Pt-I** (f), and **PS_{73}Pt-I** (g) in chloroform/methanol mixture solvent with methanol contents of 50 vol% (black), 75 vol% (red), and 90 vol% (blue).